

# Equations of state and spinodal lines – a review

N. Shamsundar and John H. Lienhard

*Heat Transfer / Phase-Change Laboratory, Department of Mechanical Engineering, University of Houston,  
Houston, Texas 77204-4792, USA*

Received 1 October 1992

Modern thermal processes in the power industry involve ever increasing heat fluxes and rapid transients. Simulating such processes requires accurate thermodynamic properties and correlations that encompass stable as well as metastable states. Here we review the development of cubic equations of state that can be made to yield very accurate thermodynamic properties of liquids in saturation and metastable (superheated) states. These cubic equations enable us to develop predictions and correlations for a number of other quantities which are either useful in themselves or for application to boiling and two-phase flow. Examples of such results include predictions of the saturation pressure, the limiting liquid superheat, the destructive energy available to a superheated liquid, the surface tension of a saturated fluid and the approach of the specific heat at constant pressure to infinity at the spinodal point. These topics are described and discussed, and it emerges that these seemingly separate topics can be unified by the use of cubic equations of state. We pay particular attention to the issue of a possible connection between the limit of liquid superheat and the liquid spinodal line.

## 1. Scope

Thermal systems are rapidly pushing toward more intense heat fluxes in more compact equipment. One result of these changes is that we shall have to operate in new regimes where our experience and accumulated data will fall us, and it becomes necessary to anticipate the performance of thermal systems on the basis of scientific theory. One of these regimes is that of metastable liquids, that is, liquids at a temperature higher than the local saturation temperature or, equivalently, at a pressure below the local saturation pressure. Such a superheated liquid state poses the threat of a serious thermohydraulic explosion following a break in a nuclear reactor coolant line, and in other accidental equipment failures. Similar problems arise when a nuclear reactor core gets rewetted, or when a liquid metal coolant leaks from a reactor and contacts other liquids. On a more benign note, a knowledge of superheated liquid properties is often needed in predicting boiling behavior.

The present review is similar to an earlier review [1], but includes important developments subsequent to it. Specifically, our new position is that a correct equation of state (EOS) is the gateway to obtaining spinodal and other derived properties, which are then used to

develop corresponding states correlations (CSC), as opposed to developing CSCs by various methods and then using these correlations in building the EOS. We also argue that it is sufficient to consider the  $p-v-T$  EOS rather than a “fundamental” (see below) EOS.

Experimental results are meager and quite hard to obtain, particularly in the neighborhood of the spinodal limit. Rapid depressurization using very clean fluids is one technique for obtaining such data, and we may cite [2], [3], [4] and [5] for some available results. Most of the available experimental data pertain to states much closer to the saturated liquid state than the spinodal limit. This review concentrates on analytical and computational techniques that do not have this limitation.

## 2. Continuous equations of state

### 2.1. Physical behavior of a hot fluid when depressurized

Let us establish the nomenclature for the rest of the paper with reference to fig. 1. This figure shows the isotherms of a real fluid on  $p-v$  coordinates. Between the saturated liquid state,  $f$ , and the saturated vapor state,  $g$ , the pressure varies non-monotonically. The

horizontal dashed line connecting  $f$  and  $g$  is what we usually see, but this line merely represents *mixtures* of saturated liquid and saturated vapor. The location of an intermediate point on the dashed line represents the composition of the mixture rather than a separate state. On the true isotherm joining  $f$  and  $g$ , pressure and volume vary continuously. As we move down from a compressed liquid state, the pressure falls rapidly

and reaches a minimum at point  $l$ , the liquid spinodal point. Beyond this point, the pressure increases, reaching a maximum at the vapor spinodal point,  $v$ , after which it falls steadily towards the ideal gas regime. The regions we have so far traversed are, in order, compressed liquid until  $f$ , metastable or superheated liquid from  $f$  to  $l$ , unstable fluid from  $l$  to  $v$ , metastable or supercooled vapor, and superheated vapor. The loci

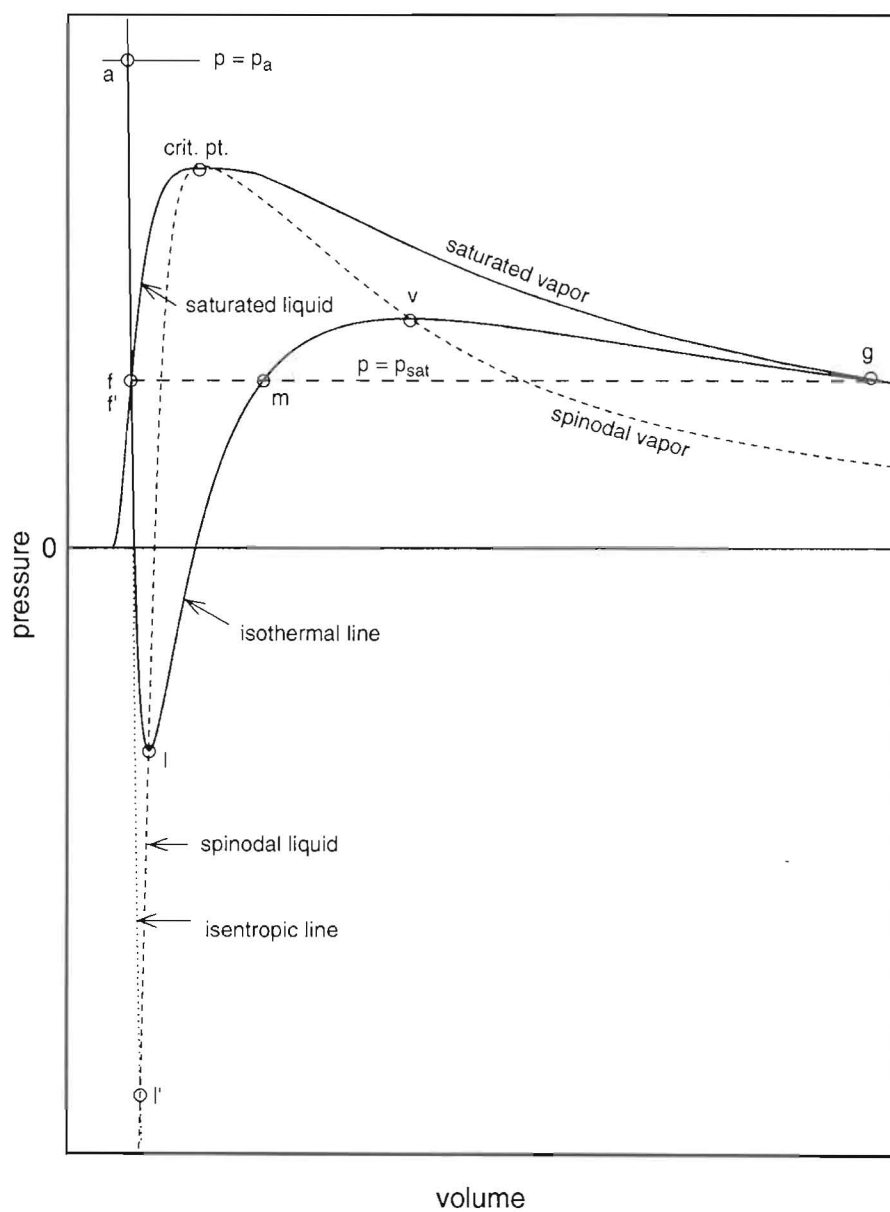


Fig. 1. Sketch of  $p$ - $v$  diagram showing real-gas isotherms and spinodal lines.

of spinodal states, shown by short dashes, are the liquid spinodal line and the vapor spinodal line, which join with the saturated liquid and saturated vapor lines at the critical point.

Every state on the isotherm is an equilibrium state, although we often encounter the incorrect adjective “nonequilibrium”, in the literature, for the states lying between  $l$  and  $v$ , and sometimes even for the metastable states. The spinodal curves are loci of  $(\partial p/\partial v)_T = 0$ .

Let us next use this figure to see what happens when we depressurize a liquid, starting with an initial state  $a$  in the compressed liquid region. Depending on the rate of depressurization, the fluid follows a process that is bounded by the isothermal and the isentropic curves, which correspond to infinitely slow and infinitely fast depressurization, respectively. Very often, these curves differ little from each other, as we can infer from the thermodynamic relations

$$\frac{(\partial p/\partial v)_s}{(\partial p/\partial v)_T} = \frac{c_p}{c_v}, \quad (1)$$

$$c_p - c_v = T v \beta^2 / \kappa_T = -T \frac{(\partial p/\partial T)_v^2}{(\partial p/\partial v)_T}.$$

If the liquid has  $v$  and  $\beta$  small enough to overcome the effect of  $\kappa_T$  being small,  $c_p \approx c_v$ . (These remarks do not hold at temperatures comparable to the critical temperature or deep within the metastable liquid region, as detailed later).

The state point of a fluid being depressurized under isothermal conditions thus moves along the segment  $a-f-l$ , and how close to the spinodal point it gets depends on two competing factors: the rate of depressurization, and the extent of the disturbances that tend to make the liquid flash into vapor. The faster the depressurization and the fewer the sources of heterogeneous nucleation, the closer can the state of the liquid come to the spinodal limit  $l$ . But the reader should bear in mind that fast isothermal processes are hard to achieve because we may be unable to supply the heat needed to maintain constant temperature in a fast process. At the other extreme, a slow process with an industrial quality liquid will vaporize very close to the saturation point  $f$ .

An isentropic depressurization process will follow the slightly different process  $a-f'-l'$ , but the remarks made in the preceding paragraph still apply. The isentropic process is a better approximation than an isothermal process to a fast depressurization process. The points  $f'$  and  $l'$  are intersections of the isentropic

line through  $a$  with the liquid saturation line and the liquid spinodal line, respectively. It is important to note that the isentropic curve *does not* have zero slope at the spinodal state  $l'$ , but does so somewhere in the unstable region.

## 2.2. The need for continuous equations of state

By continuous equation of state (CEOS) we mean  $p-v-T$  EOSs (the reasons for restricting ourselves to  $p-v-T$  equations are discussed below under “Fundamental versus  $p-v-T$  equations of state”) that represent thermodynamic data over a wide range of pressures and temperatures in the liquid state, the vapor state, the metastable states and even the unstable state. Such equations should not use any sub-regions because of the inevitable discontinuities at sub-region boundaries. This may seem too much to ask, and it is logical to question why we should look for such equations. Why should we look for an EOS that works in the unstable region, which has no practical interest? Is it not reasonable to expect that a less-constrained equation or equations might fit experimental data more accurately?

The unstable region is normally inaccessible to experiments, and the closer we wish to approach the spinodal line starting from the stable regions, the harder it is to obtain data. One of our central objectives is to obviate such experiments and to describe how metastable-state properties can be obtained by analytical methods, using only stable-state data. Therefore, the best we can hope to do in predicting metastable states in design work is to use the ample stable-state data and paltry metastable-state data, and perform extrapolation. For this extrapolation to succeed, it is essential that the equation of state should be constrained in such a way that it shows correct behavior everywhere. It should not have a form that gives it the freedom to go astray.

Continuous EOSs are not newcomers. The first equations of state were, in fact, continuous. In the 1950's and 1960's however, CEOSs were abandoned because of difficulties in applying them to common substances. The vast literature on modern equations of state (see the comprehensive books [6], [7]) contains many equations of state, some valid only for liquids, some only for vapors, and we find separate correlations for different thermodynamic properties. Such separate correlations, while convenient to use, are often inconsistent with one another (i.e., they do not satisfy the relevant thermodynamic relations). More recently, interest has returned to CEOSs.

The Keenan–Keyes–Hill–Moore equation for water [8] and the quite similar Haar equation for ammonia [9] were among the first CEOSSs, but neither of them represented the unstable region correctly, and neither was accurate in the metastable region. These equations have the form

$$p = RT/v + p_1(T, v) \quad (2)$$

that is, the pressure is the sum of an ideal gas term and a correction function  $p_1$ . This requires the correction function not only to impart accuracy to the equation. It must also impart real fluid behavior, as well. Specifically, it must characterize the change of phase. This double duty is rather onerous, and these equations fail to achieve correct behavior in the unstable region as a result.

The more recent Haar–Gallagher–Kell equation for water [10] and other equations for hydrocarbon and cryogenic fluids [11] show significantly better behavior in the near metastable region although they were not constrained to make them more accurate there. The Haar–Gallagher–Kell equation is of the form

$$p = p_0(T, v) + p_1(T, v), \quad (3)$$

where the so-called base function,  $p_0$ , represents real fluid behavior, and the correction function  $p_1$  has only to improve the accuracy of the equation. The NBS-NRC Steam Tables [12] based on the Haar–Gallagher–Kell equation represent the state of the art in thermodynamic property tables, and even include corrections to the global equations of state to account for anomalous behavior in the neighborhood of the critical point. Despite this, the Haar–Gallagher–Kell equation is not correct in the unstable region, as we shall illustrate in Section 4.2.

What, then, is the nature of a correctly behaved EOS? It should be cubic in nature, that is, it should have the form shown in fig. 1; qualitatively, it should resemble the original cubic equation of van der Waals. We say that an EOS is *cubic* if, when values are substituted for temperature and pressure into it, we have a cubic (algebraic) equation for volume. We say that an EOS is *cubic-like*, if, with values substituted for temperature and pressure, it gives only three positive roots for volume. Complicated equations such as the Haar–Gallagher–Kell equation are of such form that it is almost impossible to establish whether they are cubic-like by actually finding and counting the roots.

Such equations should meet the test of the Van der Waals theory of surface tension [13]. We shall show the results of applying this theory later, but we note here

that the Haar–Gallagher–Kell equation is not cubic-like at some temperatures, and we may establish this to be the case either by using the surface-tension theory or by examining plotted isotherms. We shall insist that any EOSs that we use should be cubic-like. Violating this requirement would give us equations that display additional stable regions surrounded by unstable regions, and this is not physically plausible (see details in Sections 4.2 and 4.8).

### 2.3. Fundamental equations versus $p$ – $v$ – $T$ equations of state

So far, we have considered only  $p$ – $v$ – $T$  equations, but a  $p$ – $v$ – $T$  equation does not furnish a complete thermodynamic description of a substance. Equations from which all thermodynamic properties can be calculated by arithmetical operations and partial differentiation are called “fundamental” or “canonical” EOSs. Four common fundamental EOSs for a pure substance take the forms  $s = s(u, v)$ ,  $h = h(s, p)$ ,  $f = f(T, v)$ , and  $g = g(T, p)$ . To see how other equations of state are obtained from a fundamental equation, consider, for example, the  $s = s(u, v)$  EOS. From this, we obtain the  $p$ – $v$ – $T$  EOS by using the relations

$$p/T = (\partial s/\partial v)_u \quad \text{and} \quad 1/T = (\partial s/\partial u)_v. \quad (4)$$

The most commonly used fundamental equations today are written in the  $f = f(T, v)$  form, which is the Helmholtz form. This fundamental EOS can be constructed by combining a  $p$ – $v$ – $T$  equation and a low pressure specific heat equation  $c_p^o = c_p^o(T)$  (this is sometimes called the “caloric equation”) to obtain

$$\begin{aligned} f(v, T) = & f_{\text{ref}} + \int_v^{RT/p_{\text{ref}}} p \, dv' \\ & + \int_{T_{\text{ref}}}^T c_p^o(T') (T/T' - 1) \, dT' - R(T - T_{\text{ref}}), \end{aligned} \quad (5)$$

where  $(p_{\text{ref}}, T_{\text{ref}})$  is a reference state at which the substance behaves as an ideal gas and the entropy is taken as zero, and primes indicate dummy variables in the integrals. The  $c_p^o(T)$  equations are well established for many substances and pose no problem. Because of these facts, we shall focus attention on  $p$ – $v$ – $T$  equations alone, but the reader should remember that, if he desires, he can always construct a fundamental EOS by using eq. (5). Most of the popular  $p$ – $v$ – $T$  equations give  $p$  as an explicit function of  $T$  and  $v$ , and the integrations in this equation can be carried out analyti-

cally. Although  $p$  and  $T$  are the most easily measured quantities, *continuous* equations explicit in these variables are impossible to develop, since we shall need multiple valued expressions. (The International Formulation Committee equations [14] did have  $p$  and  $T$  as the independent variables, but these equations were not EOSs, and apply only to the stable regions.)

### 3. A strategy for obtaining accurate cubic equations of state

The preceding considerations have led us, along with other investigators, to the conclusion that predicting metastable-state properties requires the use of an EOS with cubic-like behavior. The choice then is between true cubics and cubic-like complex expressions. Although cubic EOSs are able to depict all features of real-fluid behavior qualitatively, they do not have a good record in representing data with high accuracy. Indeed, this is the case if cubic equations are fitted to data in the usual way, in which the forms of the temperature dependence of the coefficients are set *a priori*, and the values of the coefficients are then found by regression.

We choose to fit the cubics in a completely different way, a way that our intuition tells us should fail. The method succeeds beyond our expectations, and most of our objectives can be met without moving on to more complex equations.

The method applies only to subcritical temperatures, and is as follows.

- (1) We fit the cubic equation isotherm by isotherm. This feature is what sets our cubic apart from others, and we shall call an equation so fitted as a *T-cubic*.
- (2) At each subcritical temperature, we use a minimum number of stable-state data, enforce thermodynamic constraints, and find the coefficients of the cubic in a deterministic way rather than by statistical methods.
- (3) We now have tables of the coefficients of the cubic as functions of  $T$ . We consider the T-cubic equation to have coefficients represented as tables, and calculate other derived properties. Some of these are available independently and, therefore, serve to examine the accuracy of the cubic equation, whereas the rest constitute predicted properties for use elsewhere.

Let us now display the cubic equation and the method for calculating its coefficients. The very form of the equation is suggested by considering the curve

$f-l-m-v-g$  in fig. 1. This curve intersects the horizontal line  $p = p_{\text{sat}}$  at the points  $f$ ,  $m$  and  $g$ ,  $m$  being the intermediate point in the unstable region, to which we attach no other physical significance. The shape of the figure tells us that a cubic-like equation must be of the form

$$\frac{p}{p_{\text{sat}}} = 1 - \frac{(v - v_f)(v - v_m)(v - v_g)}{F(v)}. \quad (6)$$

For the equation to be cubic-like,  $F(v)$  should have no poles or roots in the physical range of  $v$ , which is from the smallest specific volume for compressed liquid out to infinity. For the equation to be a true cubic,  $F(v)$  should at the most be cubic in  $v$ , but satisfying the ideal-gas limit correctly requires that  $F(v)$  indeed be cubic, and have  $v^3$  as the leading term. The final form of the cubic equation is

$$\frac{p}{p_{\text{sat}}} = 1 - \frac{(v - v_f)(v - v_m)(v - v_g)}{(v - b')(v^2 + 2c'v + d')}. \quad (7)$$

The quadratic expression in the denominator may have real or complex factors. In the former case, we need to verify that no pole lies in the physical range of  $v$ .

The cubic equation contains seven parameters, all of which are functions of temperature. Among these,  $p_{\text{sat}}$ ,  $v_f$  and  $v_g$  are obtained either directly from data or, more commonly, from complex EOSs such as the Haar-Gallagher-Kell equation. In addition, there are two thermodynamic constraints to be satisfied. The first is the ideal-gas limit, which requires that  $\lim_{v \rightarrow \infty} pv/RT = 1$ . It yields

$$-b' + 2c' + v_f + v_m + v_g = RT/p_{\text{sat}}. \quad (8)$$

The second condition is the Gibbs-Maxwell condition,

$$\int_{v_f}^{v_g} p \, dv_T = p_{\text{sat}}(v_g - v_f), \quad (9)$$

which makes the Gibbs function  $g = h - Ts$  the same for vapor and liquid in equilibrium.

We now have two degrees of freedom left in choosing the coefficients of the cubic equation. Since the metastable liquid is of great interest to us, we shall impose both the two needed constraints on the liquid side. One of these is the isothermal compressibility  $\kappa_T$  of saturated liquid, and the other is a single compressed-liquid point  $a$  at a rather high pressure,  $p_a$ . If we think of bending an elastic strip into the shape of the isotherm on  $p-v$  coordinates, we see that choosing

more constraints on the liquid side is equivalent to using greater leverage on that side.

The integral in the Gibbs–Maxwell condition (9) can be evaluated analytically, and the resulting set of equations for the coefficients  $b'$ ,  $c'$ ,  $d'$  and  $v_m$  are nonlinear. However, it is not necessary to solve for these coefficients simultaneously. For an assumed value of  $b'$ , the other coefficients can be computed explicitly, and the Gibbs–Maxwell condition becomes the test for the correctness of  $b'$ . Therefore, a simple one-variable root finding method such as the secant method is adequate for finding  $b'$  and the remaining coefficients.

### 3.1. Reduced variables and property preserving volume transformations

In proceeding further with the cubic equation, we work with a nondimensional form of it in which we employ the usual reduced variables  $p_r \equiv p/p_c$ ,  $T_r \equiv T/T_c$  and an unconventional volume variable  $r \equiv (v/v_c - 1)Z_c$ . As shown by Shamsundar and Reddy [15], the use of  $r$  instead of the conventional  $v$ , has the following advantages. The critical point corresponds to  $r = 0$ , any equation of state must asymptotically behave as the equation  $r^3 = 0$ , and using the critical point as the origin is logical from the physical point of view. Next, the equations used to represent the ideal gas limit, the critical point conditions, the Gibbs–Maxwell condition and the spinodal state become independent of  $Z_c$  (however, the surface tension equation does not show the same independence). The cubic equation (7) in these new variables is

$$\frac{p_r}{p_{r,\text{sat}}} = 1 - \frac{(r - r_f)(r - r_m)(r - r_g)}{(r + b)(r^2 + 2cr + d)}, \quad (10)$$

where  $b$ ,  $c$  and  $d$  are obtained from  $b'$ ,  $c'$ ,  $d'$  by equating the right hand sides of equations (7) and (10).

Shamsundar and Reddy showed that if a cubic or other equation of state is transformed from its usual  $p_r-v_r-T_r$  form to the  $p_r-r-T_r$  form and then back to the  $p_r-v_r-T_r$  form with a different  $Z_c$ , then the resulting equation has the same reduced vapor-pressure as the original equation. They used this invariance property to show how the well-known Soave–Redlich–Kwong equation [16], which has  $Z_c = 1/3$ , can be made to yield good values for the saturated liquid volumes of water ( $Z_c = 0.233$ ) and ammonia ( $Z_c = 0.246$ ) – polar fluids for which this equation is not considered suitable and modifications have been advanced [17]. They also presented corresponding-states plots of  $r_g$  against the Pitzer factor,  $\omega$ . (This factor has been established to be a better choice than the critical compressibility factor,

$Z_c$ , in obtaining corresponding-states correlations of the properties of fluids [18].) These plots showed considerably better correlation than plots of  $v_{rg}$  against  $\omega$ . In general, if most of the predicted properties are accurate but the predicted volumes are inaccurate, these predicted volumes can be improved by using the volume transformation.

## 4. Some results of fitting the cubic equation of state to common fluids

### 4.1. The coefficients of the cubic for water

Murali [20], Biney [21], Vandermarliere [22] and Reddy [23] generated input data for the cubic equation (10) for about 20 substances using the best available complex equations of state ([11,12] and the compilation of Reynolds [19]), at about 50 reduced temperatures ranging from 0.46 to 0.99. The resulting coefficients were plotted against  $T_r$  and against  $1/T_r - 1$ . It quickly became clear that the coefficients varied in a complicated and sometimes non-monotonic way, and therefore there is no hope of fitting simple explicit expressions in terms of  $T_r$  for the coefficients  $b$ ,  $c$ ,  $d$  and  $r_m$ . As an example, we show plots of  $b$ ,  $c$ ,  $d$ , and  $r_m$  in fig. 2.

### 4.2. Comparison of the cubic to other cubics and complex equations

Murali [20] worked with a simpler form of eq. (10). He assumed that he could set  $d = c^2$  and he did not

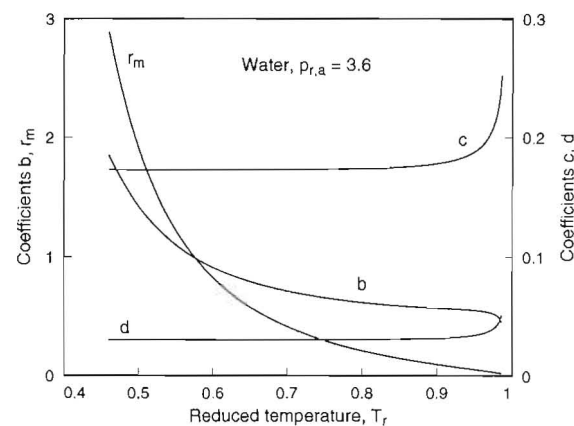
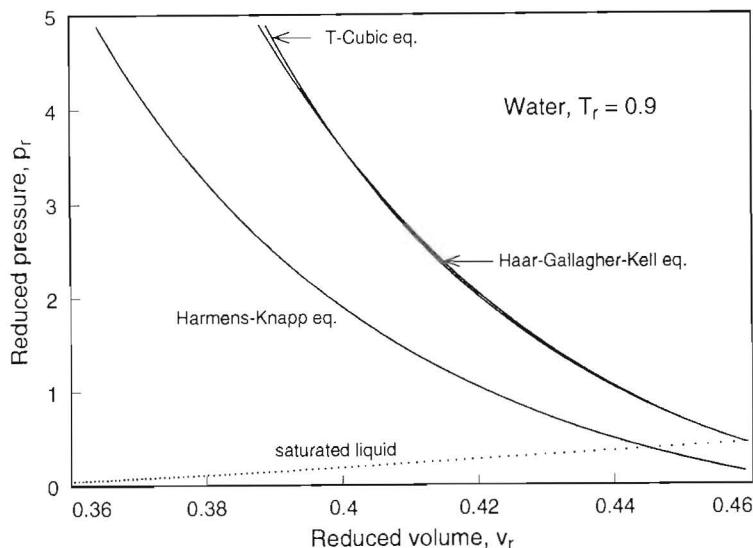


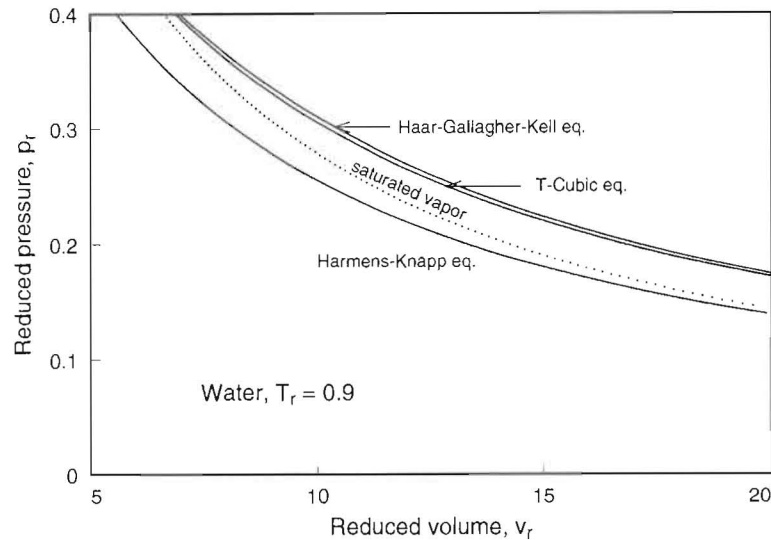
Fig. 2. Temperature-dependence of coefficients of T-Cubic for water.

Fig. 3. Comparison of isotherms for liquid water at  $T_r = 0.9$ .

use any compressed liquid data in fitting the equation. He made extensive comparisons with existing cubic equations, and concluded that the T-cubic was far superior to other cubic equations in representing compressed liquid and metastable states.

Biney [21] extended Murali's work by using the full form of the T-cubic equation. He used the Haar-Gal-

lagher-Kell equation to generate the input data for the T-cubic equation, and computed various secondary properties such as saturation and spinodal pressures, speed of sound and surface tension with the cubic equation. He used all this information to refit the Haar-Gallagher-Kell equation so as to obtain improved behavior in the metastable and unstable re-

Fig. 4. Comparison of isotherms for steam at  $T_r = 0.9$ .

gions, but found that this was at the expense of reduced accuracy at supercritical temperatures. In this last respect Biney's work parallels a similar effort made earlier by Karimi [24] to make such improvements to the Keenan–Keyes–Hill–Moore equation.

Biney compared the predictions of the cubic to the IFC skeleton tables for steam for temperatures ranging from 0°C to 350°C and pressures up to 1000 MPa, and concluded that the deviations were of the same order as the tolerance of the skeleton tables. A comparison of the cubic equation to data and a conventional cubic equation on a  $p_r$ - $v_r$  diagram is shown in figs. 3 and 4. In these figures we show the isotherms of water at  $T_r = 0.9$  and, for reference, the saturation line. In addition to the data from the Haar–Gallagher–Kell equation and the predictions of the T-cubic equation fitted to the same data, we show one of the best three-parameter (these parameters are  $p_c$ ,  $T_c$ , and the Pitzer factor,  $\omega$ ) cubic equations available, namely, that of Harmens and Knapp [25].

The T-cubic is remarkably better on the liquid side, but it does have a flaw on the vapor side – a flaw that is a direct consequence of our imposing more constraints on the liquid side than the vapor side. This flaw is the price we pay for the excellent performance of the T-cubic in the stable liquid region and the

metastable liquid regions. In the vapor region, the T-cubic isotherm is consistently below the data, although the difference is barely noticeable. But other properties such as  $u$ ,  $h$ ,  $s$  must be computed by integration from the ideal-gas limit towards decreasing volumes, and this can result in unacceptably large cumulative errors in  $u$ ,  $h$ ,  $s$  on the liquid side. Such use of the T-cubic should be avoided. If  $u$ ,  $h$ ,  $s$  are needed for the liquid, it is far better to use the liquid at the triple point as the reference state rather than the ideal gas limit.

Another useful comparison of the T-cubic can be made to the Haar–Gallagher–Kell equation for water. The complete isotherm of water at  $T = 400^\circ\text{C}$ , as given by the Haar–Gallagher–Kell equation and by the T-cubic derived from the same equation, are displayed in the  $p$ - $v$  diagram of fig. 5. The Haar–Gallagher–Kell equation displays two maxima and two minima between the saturated liquid and saturated vapor states, and reaches extremely large positive pressures in this region. Of course, we should remember that the Haar–Gallagher–Kell equation was neither constrained nor claimed to behave correctly inside the vapor dome. In the stable and the near-metastable regions, the T-cubic and the Haar–Gallagher–Kell equation agree very well.

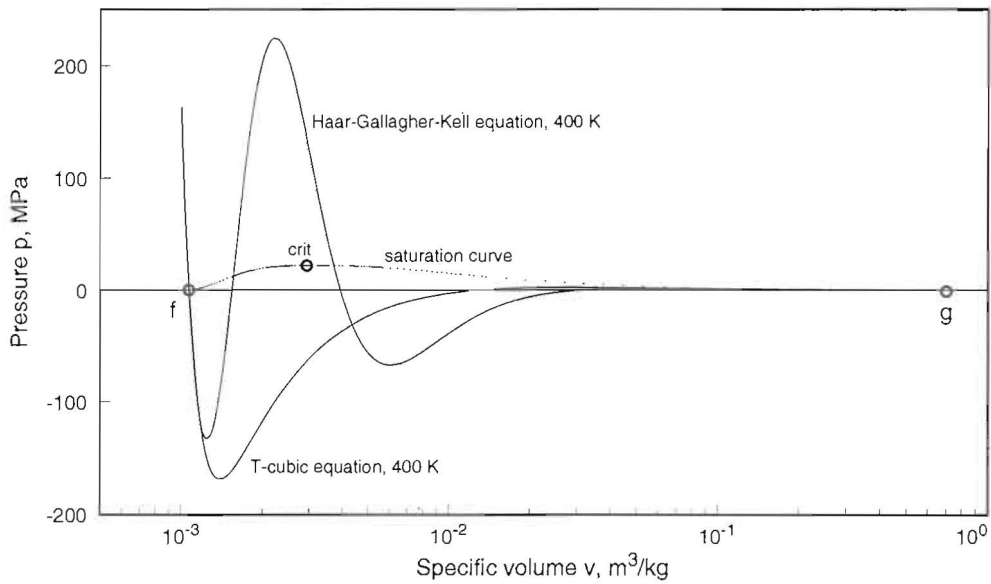


Fig. 5. Comparison of T-cubic with Haar–Gallagher–Kell equation at  $T = 400\text{ K}$ .

#### 4.3. A global cubic equation of state

Vandermarliere [22] succeeded in using high-order rational functions in  $T_r$  to represent the temperature dependence of the T-cubics. He rewrote eq.(10) in the equivalent form

$$p_r = \frac{T_r - a}{r + b} + \frac{a(r + c) + e}{r^2 + 2cr + d} \quad (11)$$

and fitted rational functions in  $T_r$  to the coefficients  $a$ ,  $b$ ,  $c$ ,  $d$  and  $e$ . He then performed a series of computationally expensive regressions to slightly improve the agreement of the resulting  $p-v-T$  equation with the data. This improvement results because, in the first

step, the deviation of the rational function fitted to the coefficients was minimized. Doing so is not quite the same as minimizing the deviation of the predicted properties. The second step closes this gap. Vandermarliere's final  $p-v-T$  equations contain 50 to 90 coefficients, and he provides values of the coefficients for seventeen different fluids. The advantages of using this form are that the equation is analytic, and at a fixed temperature the equation is a simple cubic. The results calculated from the equation usually deviate from the input data by an order of magnitude less than the tolerance in the data themselves, and this is a property shared by Vandermarliere's equations with the T-cubics. The disadvantage is the large number of

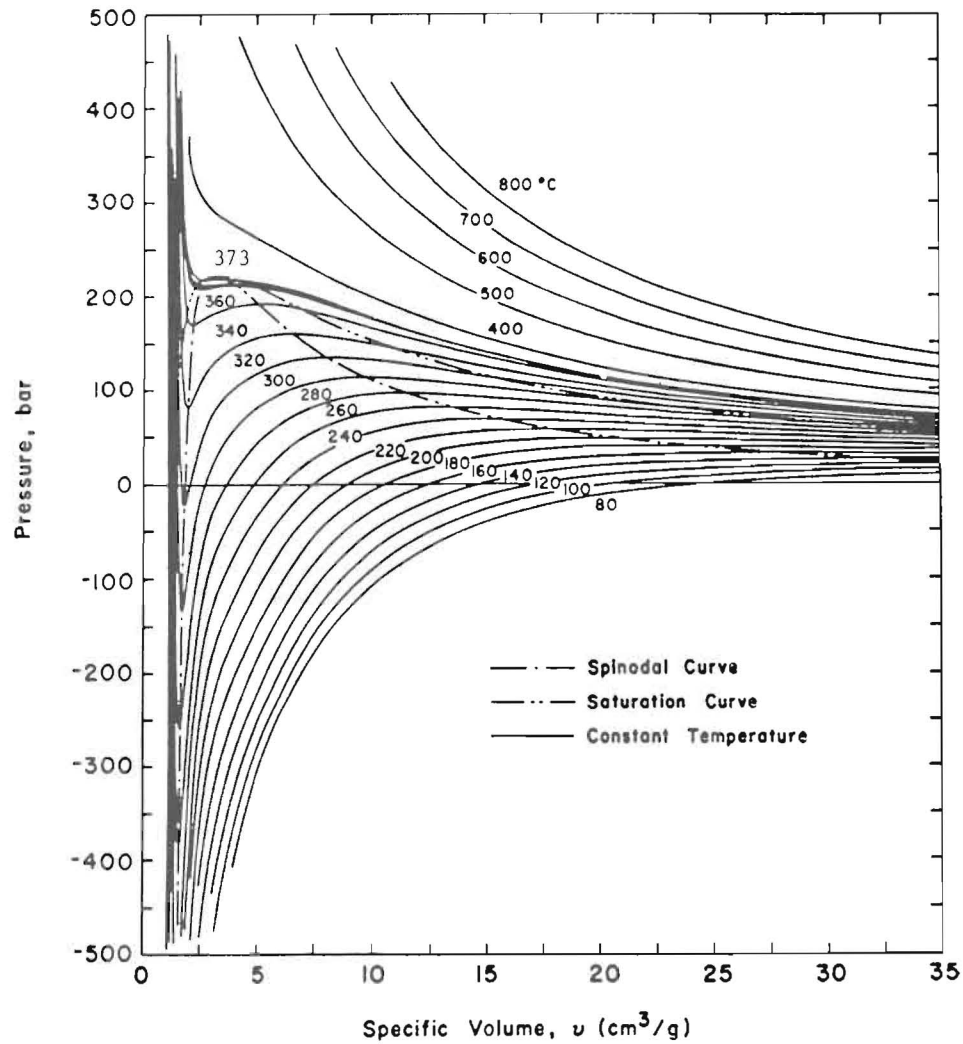


Fig. 6.  $p-v-T$  diagram for water from Biney's fundamental EOS.

coefficients. We feel that computing and storing a table of coefficients at the beginning of some complex computation that needs metastable state properties and directly interpolating in this table at a desired temperature, on the fly, is a better approach, since such equations will be used in a computer program anyway.

Vandermarliere showed that Murali's assumption that  $c^2 = d$  is satisfied very closely by the coefficients he calculated, but that allowing even a small difference between  $c^2$  and  $d$  significantly improves the accuracy of the predicted pressures in the compressed liquid and metastable liquid regions.

Vandermarliere's work is also restricted to the subcritical region.

#### 4.4. A generalized cubic equation of state

Reddy [23] extended Vandermarliere's work into the supercritical region. In fitting T-cubics to supercrit-

ical isotherms, of course, he could not use the same method as for subcritical isotherms, since there are no saturation states. He tried out a statistical method, but found that the least-squares problem was degenerate because the properties in this region often deviate little from ideal-gas behavior. The resulting coefficients varied with temperature in an unacceptably erratic way. Reddy therefore decided to require supercritical T-cubics to satisfy three constraints:

- The specific volume and  $\kappa_T$  should match data at a selected high pressure (he chose 5 times the critical pressure).
- The specific volume should match data at the critical pressure.

In addition, the T-cubic should satisfy the ideal gas limit exactly, but this is already built into eq. (11). This leaves two free coefficients in eq. (11). Reddy found these by using a locally-developed nonlinear least-squares method.

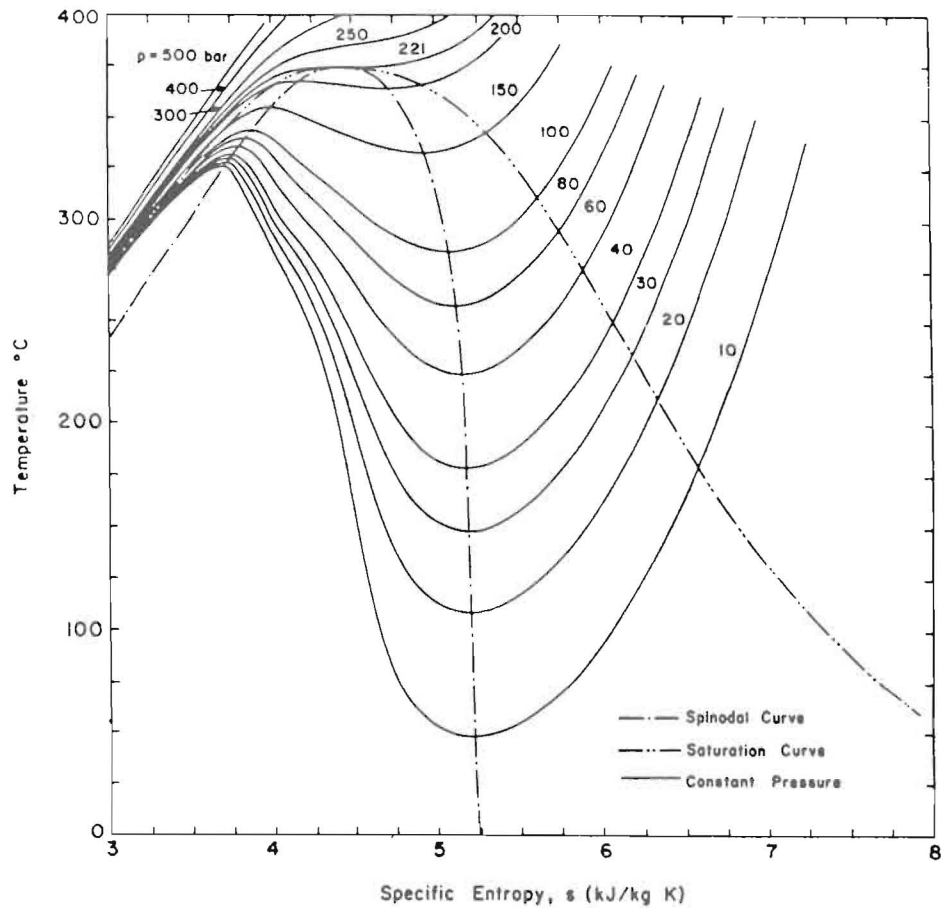


Fig. 7.  $T-s-p$  diagram for water from Biney's fundamental EOS.

After fitting T-cubics to supercritical and subcritical isotherms, Reddy fitted rational functions in  $1/T_r - 1$  to the coefficients  $a, b, c, d$  and  $e$ , but found it mandatory to use separate fits for the subcritical and the supercritical regions. This will, doubtless, cause some discontinuities in properties at the critical temperature, but this is a problem for resolution in the future.

Reddy found that the resulting global cubic equation showed deviations from data that were comparable to the tolerances in the input data, although the deviations were much higher than those achieved by Vandermarliere. Thus, it appears that the price to be paid for extending the equation to supercritical temperatures is bearable.

Reddy went further and developed a generalized cubic equation, using data for 20 substances. He fitted the T-cubic coefficients using the equation

$$C(\tau, \omega) = c_0 + c_1\omega + \frac{\sum_{i=1}^n \sum_{j=0}^4 c_{ij}\tau^i\omega^j}{1 + d_0\tau}, \quad (12)$$

where  $C$  is one of the coefficients  $a, b, c, d$  and  $e$ , and  $\tau = 1/T_r - 1$ . The upper limit in the first summation in this equation,  $n$ , is 4 for subcritical temperatures, and 3

for supercritical temperatures. Reddy was able to fit the data by fixing  $d_0$  at 40 for subcritical temperatures and zero for supercritical temperatures. In addition, he required the equation to satisfy the critical point constraints.

The resulting generalized cubic equation has 104 coefficients in the subcritical region and 79 coefficients in the supercritical region. These are higher numbers than for existing generalized cubic equations, but they increase the accuracy. In contrast to most generalized cubics, Reddy's equation applies to polar and to non-polar substances without change.

#### 4.5. A new fundamental equation of state for water

Some of the important results obtained by Biney from his fundamental equation are the modified  $p-v-T$  and  $T-s-p$  diagrams in fig. 6 and fig. 7. Note that all of the properties can be seen in these diagrams to change continuously from the liquid region to the vapor region, and the conventional straight-line representations in the "two-phase" region are not shown. The first of these figures should be compared to fig. 1. The second, the  $T-s-p$  diagram, does not show the discontinuities that were reported in the earlier review paper [1] and observed in the neighborhood of 200°C by Karimi [24]. This figure shows the spinodal lines and the

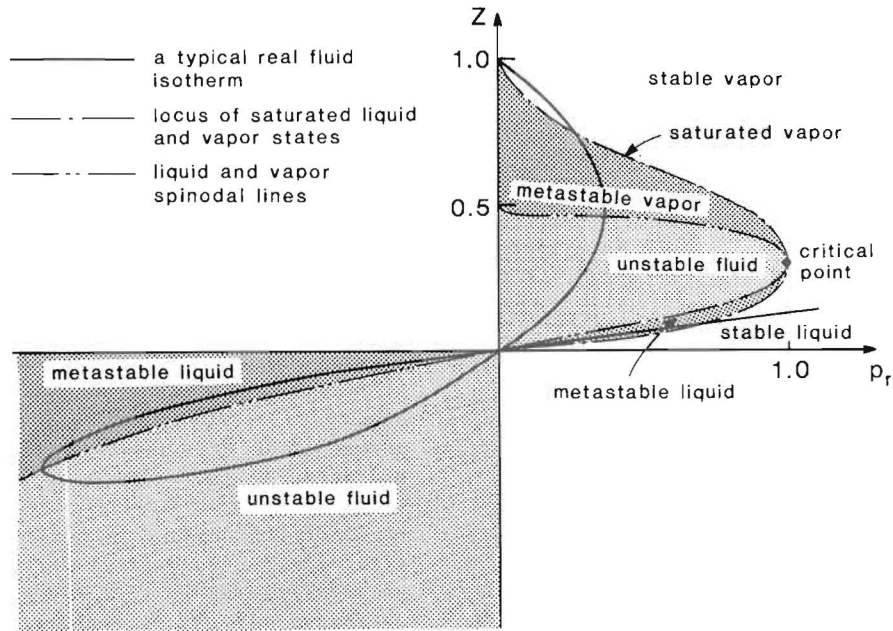


Fig. 8. Sketch of metastable and unstable regions in  $Z'$ - $p_r$  coordinates.

metastable regions in a view that complements fig. 1. However, we suspect some inaccuracy on the unstable liquid side in fig. 7 since the isobars in this region lack the smoothness we expect to find in nature.

#### 4.6. A modified compressibility chart for water and other substances

Dong and Lienhard [27] used the cubic equation (10) to generate plots of spinodal lines and various isotherms in compressibility charts. Figure 8 is a sketch which should help in understanding the next three figures, Figs. 9, 10, and 11, which are all taken from their paper. Note that in figs. 9 and 11 all the data points, except perhaps those of water, are quite close to one another (the reason for the water data deviating is that water has  $\omega$  much higher than most of the other fluids shown). Therefore, fig. 11 can be used to locate the spinodal point on a  $p$ - $v$  diagram quite accurately. The spread in  $Z$  is much less over all states than the spread in either  $\omega$  or  $Z_c$ .

#### 4.7. A corresponding-states correlation for vapor pressure

In their paper [27], Dong and Lienhard also give a corresponding-states correlation for saturation pressure that, while simpler than the well-known Lee-Kesler correlation [28], agrees better with the data for many substances at lower temperatures and is significantly better for liquid metals, which have large, negative values of  $\omega$ . This new correlation, which fits 634 data points obtained from reported data or equations

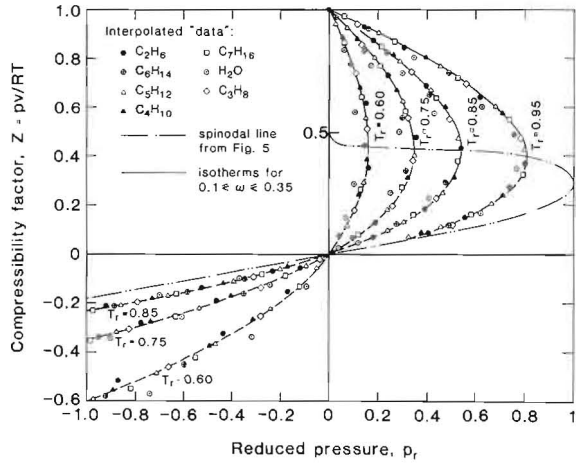


Fig. 9. Z-chart of metastable and unstable isotherms for many substances.

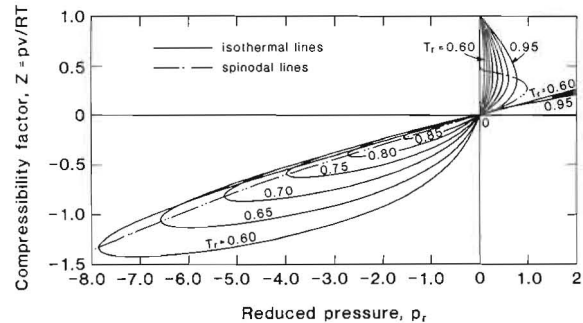


Fig. 10. Z-chart of metastable and unstable isotherms for water.

in [6, 19, 29] with an r.m.s. accuracy of  $\pm 0.42$  percent in  $T_r$ , is

$$\begin{aligned} \ln p_{r,\text{sat}} = & 5.37270(1 - 1/Tr) \\ & + \omega(7.49408 - 11.18177Tr^3 + 3.68769Tr^6 \\ & + 17.92998 \ln T_r). \end{aligned} \quad (13)$$

We display in fig. 12 a comparison of the data used to develop eq. (13) with the values computed from this equation and from the Lee-Kesler equation.

#### 4.8. Surface tension of saturated fluids

The exact relation between the surface tension of a saturated fluid and the  $p$ - $v$ - $T$  equation was derived in 1894 by Van der Waals [13] based on theoretical considerations. This relation is

$$\frac{\sigma}{\sigma_0} = \int_{v_f}^{v_g} \left[ \frac{\int_{v_f}^v (p_{\text{sat}} - p) dv'}{v^5} \right]^{1/2} dv. \quad (14)$$

Both the integrals in this equation are carried out along an isotherm. The factor  $\sigma_0$  is an unknown quantity which can, in principle, be obtained from a knowledge of the molecular structure. But, for all practical purposes, it has to be found by matching this equation to data. As we stated earlier, this equation is a very stringent test of an equation being cubic-like. If an equation is not cubic-like, the subexpression  $\int_{v_f}^v (p_{\text{sat}} - p) dv'$  will become negative at some values of  $v$  in the unstable region and the evaluation will fail. Even if an equation is cubic-like, the calculated temperature-dependence of surface tension will not be accurate if the

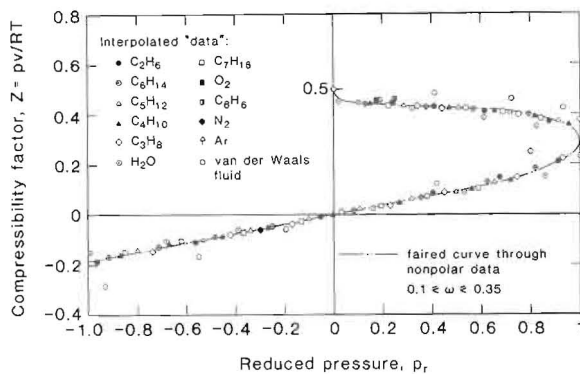


Fig. 11. Z-chart of vapor and liquid spinodal lines.

equation is not itself accurate in the unstable region. And there is no other way to examine this accuracy.

Biney, Dong and Lienhard [30] applied this equation, using T-cubics (which were fitted using data from the complex equations cited earlier) to evaluate the integrals. Using the calculated table of  $\sigma/\sigma_0$ , they performed a regression to find the value of  $\sigma_0$  that best matched surface tension-temperature data. Figure 13 shows a plot of  $\sigma/\sigma_0$  against  $T_r$  for water. The authors conjectured that the disagreement at temperatures below  $T_r = 0.5$  ( $T = 50^\circ\text{C}$ ) could be an indication of the T-cubic equation being inaccurate at such tem-

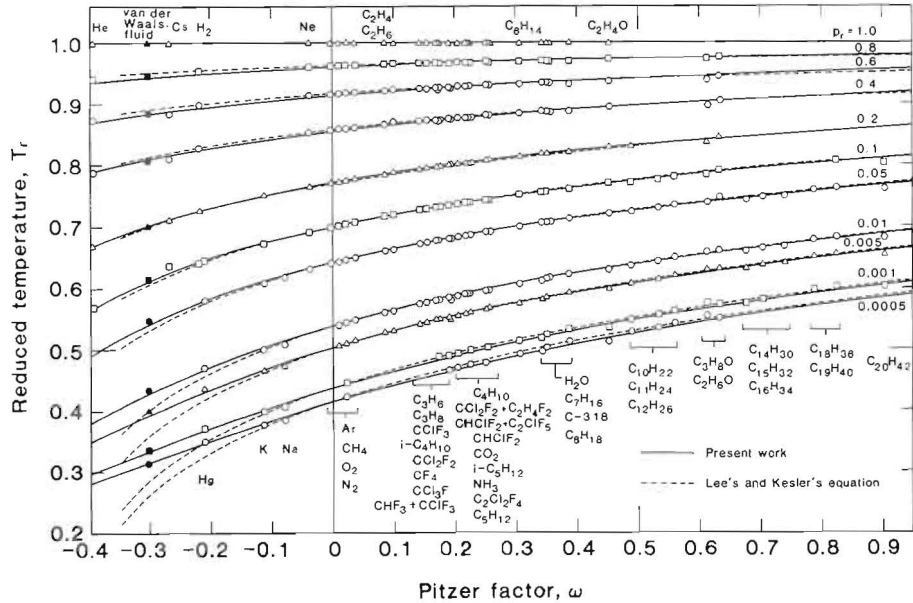
peratures – temperatures where water displays many anomalies. Similar plots for three hydrocarbon fluids and a CSC for  $\sigma_0$  are given in their paper.

### 5. The spinodal point compared to the homogeneous nucleation limit – The approach of $c_p$ to infinity at the spinodal point

Lienhard and Karimi [31] argued that the highest attainable homogeneous nucleation temperature for a liquid at a given pressure,  $T_n$ , is extremely close to the liquid spinodal temperature,  $T_s$ . They did this by comparing the thermodynamic availability of the spinodal liquid (referred to the homogeneous nucleation point at the same pressure) with the disturbance energy of molecular fluctuations at the spinodal temperature. This availability,  $a$ , is given by

$$\begin{aligned} a &= \int_n^l d(h - T_n s)_p = \int_n^l (T - T_n) ds_p \\ &= \int_{T_n}^{T_l} c_p \left( 1 - \frac{T_n}{T} \right) dT. \end{aligned} \quad (15)$$

There was a problem with their comparison, because  $c_p$  tends to infinity as the spinodal points are approached, as we can see from eq. (1) by noting that  $(\partial p/\partial v)_T = 0$  at the spinodal point. They did not know



how  $c_p$  approaches infinity, and assumed a variation of the type

$$c_p = \frac{A(p)}{(T_l - T)^n} \quad (16)$$

with the coefficient  $n$  such that  $0 \leq n < 1$ . Lienhard and Karimi guessed the exponent  $n$  to be almost equal to 1, and estimated the integral in eq. (15). Thus they concluded that  $a$  was given by

$$a < D c_p(T_n) \frac{(T_l - T_n)^2}{T_l}, \quad (17)$$

where  $D$  is a number larger than unity. In this section, we shall replace these conjectures by precise statements, and then infer the relation between  $T_n$  and  $T_l$ .

### 5.1. The temperature dependence of $c_p$ along an isobar

The first task is to find out exactly how  $c_p$  tends to infinity as the spinodal point is approached. To do so, we write eq. (1) in the equivalent form in reduced variables

$$\frac{c_p - c_v}{R} = -Z_c T_r \frac{(\partial p_r / \partial T_r)^2}{(\partial p_r / \partial v_r)} = -T_r \frac{(\partial p_r / \partial T_r)^2}{(\partial p_r / \partial r)}. \quad (18)$$

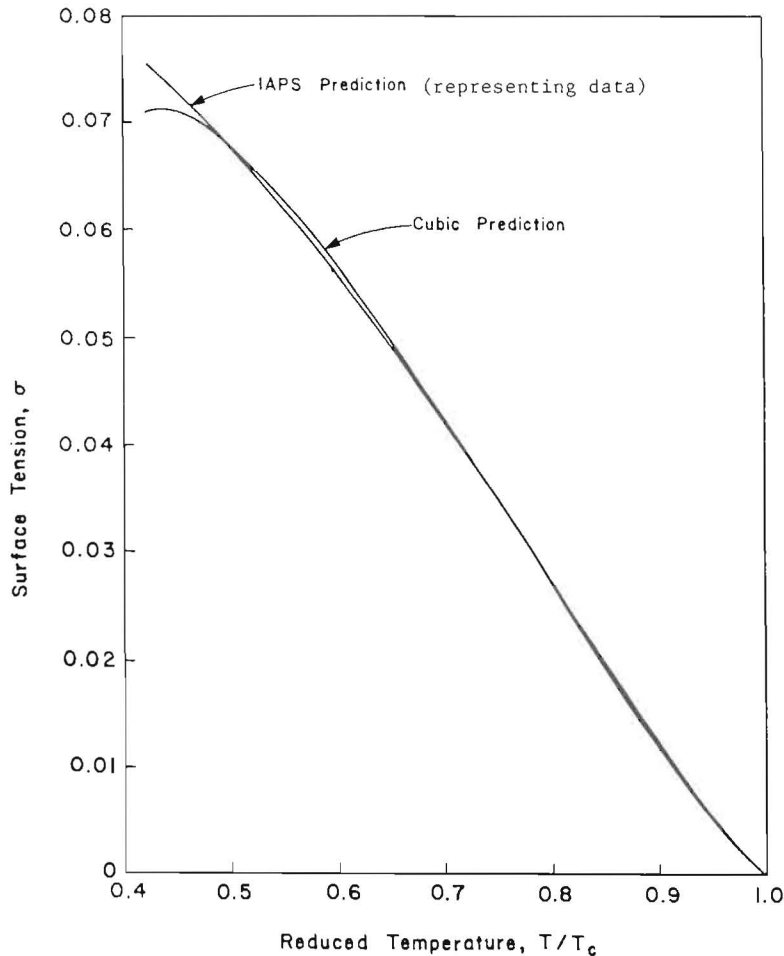


Fig. 13. Surface tension variation of water with temperature.

Next, we perform Taylor series expansions of the quantities in this equation about the liquid spinodal point. First, holding  $p_r$  fixed, we expand  $T_r$  to get

$$T_r - T_{r,l} = (\partial T_r / \partial v_r)_l (v_r - v_{r,l}) + \frac{1}{2} (\partial^2 T_r / \partial v_r^2)_l (v_r - v_{r,l})^2 + \dots \quad (19)$$

Next, we hold  $T_r$  fixed and expand  $(\partial p_r / \partial v_r)$  to obtain

$$(\partial p_r / \partial v_r) = (\partial p_r / \partial v_r)_l + (\partial^2 p_r / \partial v_r^2)_l (v_r - v_{r,l}) + \dots \quad (20)$$

At the spinodal point, the first order derivatives on the right-hand sides of the last two equations vanish. From the first of this pair of equations, we note that  $(v_r - v_{r,l})$  varies as the square root of  $(T_{r,l} - T_r)$ . We then solve for  $(v_r - v_{r,l})$  from it and substitute the result into the second equation and solve for  $(\partial p_r / \partial v_r)$ . This result, when substituted into the denominator of eq. (18), gives

$$\frac{c_p - c_v}{R} = Z_c T_{r,l} \frac{(\partial p_r / \partial T_r)_l \sqrt{-(\partial^2 T_r / \partial v_r^2)_l}}{(\partial^2 p_r / \partial v_r^2)_l \sqrt{2(T_{r,l} - T_r)}}. \quad (21)$$

We then note that  $c_v$  remains finite everywhere, whereas  $c_p$  is far greater in the near-spinodal region. Thus, we get the asymptotic formula

$$\frac{c_p}{R} = \frac{A(p_r)}{(T_{r,l} - T_r)^{1/2}} \quad (22)$$

with the function  $A(p_r)$  given by (after transforming some of the derivatives in eq. (21) into a more convenient form for use with a pressure-explicit EOS)

$$A(p_r) = T_{r,l} \frac{(\partial p_r / \partial T_r)_l^{3/2}}{(2\partial^2 p_r / \partial r^2)_l^{1/2}}. \quad (23)$$

The partial derivatives in this expression are all evaluated at the liquid spinodal point.

We have evaluated  $A(p_r)$  for a number of fluids over the full range of pressures, by fitting T-cubics as in the preceding section and evaluating the derivatives with the T-cubics. The derivative  $(\partial^2 p_r / \partial r^2)_l$  is evaluated analytically from the T-cubic, but  $(\partial p_r / \partial T_r)_l$  must be computed numerically. At liquid spinodal pressures below  $p_r = 0.1$ , we found that  $A(p_r)$  changed insignificantly with  $p_r$ . For our purposes, we deem it sufficient to take  $A(p_r)$  to be constant and evaluate it at  $p_r = p_l = 0$ . We shall call this value  $A_0$ . The computed values of  $A_0$  are plotted against  $\omega$  for a number of substances in fig. 14. For comparison purposes, we show the curve for the Soave equation [16], and the point for the

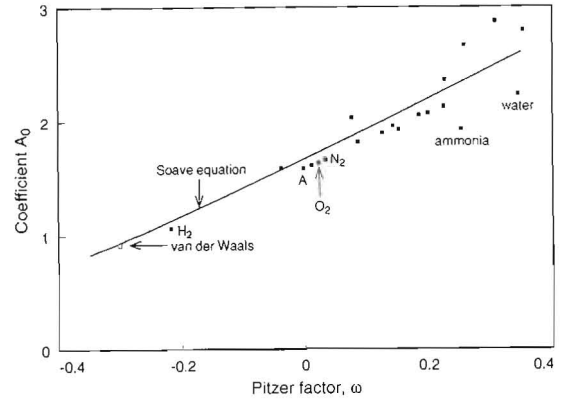


Fig. 14. Corresponding states plot of coefficient  $A_0$ .

remarkable van der Waals equation falls on this curve, too. There is fairly good correlation between  $A_0$  and  $\omega$ , and  $A_0$  lies between 1.5 and 3 for most substances. A least-squares linear fit is

$$A_0 = 1.69 + 2.54\omega. \quad (24)$$

An exploratory calculation made directly with complex equations of state produced far greater scatter, but even those values of  $A_0$  lay between 1 and 2. Thus eq. (24) serves us quite well in the order of magnitude estimates below.

### 5.2. Prediction of the minimum value of $T_l - T_n$

Equations (22) and (24) make it possible to obtain an improved estimate of the limiting value of  $T_l - T_n$ . The strategy for doing this is to compare the availability,  $a$ , given in eq. (15) with the critical work or "potential barrier" required to create a nucleus bubble,  $\Delta G$  (see, e.g. [32]). If  $a$  times the mass of the molecules participating in the nucleation event is less than  $\Delta G$ , any homogeneous disturbance large enough to trigger nucleation will first put the liquid past the spinodal limit. We therefore look for the value of  $T_l - T_n$  for which these quantities are just equal.

First, we calculate the availability  $a$  by using eqs. (22) and (24) in eq. (15). The integral can be computed exactly, and we obtain

$$\frac{a}{RT_c} = A_0 \left[ 2\sqrt{T_{r,l} - T_{r,n}} - \frac{T_{r,n}}{\sqrt{T_{r,l}}} \ln \left( \frac{T_{r,l} + \sqrt{T_{r,l} - T_{r,n}}}{T_{r,l} - \sqrt{T_{r,l} - T_{r,n}}} \right) \right]. \quad (25)$$

We may simplify this result for the case  $T_{r,l} - T_{r,n} \ll 1$  to obtain

$$\frac{a}{RT_c} = \frac{4}{3} A_0 \left( 1 - \frac{T_{r,n}}{T_{r,l}} \right)^{3/2}. \quad (26)$$

Next, we draw upon nucleation theory (see [32] or [5]) to find  $\Delta G$ . The theory tells us that the ratio,  $j$ , of the number nucleation events to the number of molecular collisions, is given as  $j = e^{-\Delta G/kT_n}$ . Consider  $N$  molecules, each of mass  $m$ , taking part in a nucleation event. The availability of these molecules is  $aNm$ . This availability should equal  $\Delta G$  for nucleation. Using eq. (26) for  $a$ , we conclude that

$$\frac{4}{3} RT_c A_0 N m \left( 1 - \frac{T_{r,n}}{T_{r,l}} \right)^{3/2} = -kT_n \ln j. \quad (27)$$

Now,  $mR$ , the gas constant per molecule, is equal to  $k$  and, on average, we must have  $N = 1/j$ . Thus, we can simplify this equation to get the final result

$$\frac{4}{3} A_0 N \left( 1 - \frac{T_{r,n}}{T_{r,l}} \right)^{3/2} = T_{r,n} \ln N. \quad (28)$$

We are now able to calculate the nucleation temperature limit for water at low pressures. From fig. 14 we get  $A_0 = 2.23$  for water. The work of Dong and Lienhard [27] clearly shows that the limiting value of  $j$  for homogeneous nucleation is consistently on the order of  $10^{-5}$ . This value is consistent with the experimental results of Skripov and his co-workers [5].

From the T-cubic equation fitted to water, we compute the spinodal temperature at 1 atm as  $T_l = 602.3$  K. After substituting these quantities and the value for  $T_c$  in the preceding equation, we solve for  $T_n$  to get its value as 601.6 K. Thus, the nucleation temperature in water at moderate pressures is lower than the liquid spinodal temperature by less than 1 K. At higher pressures or higher values of  $N$ ,  $A$  and  $T_l$  both increase, and this temperature difference becomes still smaller.

Thus, we may conclude that on the liquid side, the limit of homogeneous nucleation is very close to the liquid spinodal line. For practical purposes, the two may be considered one-and-the-same.

On the vapor side, however, the available energy required to hurdle the potential barrier must be supplied by a far smaller set of particles, since a dense droplet is being created out of dispersed molecules. Nucleation must therefore occur much farther from

the spinodal limit. Lienhard and Karimi [33] showed this to be true by empirical correlation, and they made a similar analysis to the present one but without the help of eq. (22) in a subsequent paper [31].

### 5.3. Depressurization of hot liquids and their damage-potential

Correlations were given in the earlier review [1] for the pressure undershoot (below saturation) of rapidly depressurized hot water and the rate of depressurization. Plots of the undershoot for various depressurization rates and initial temperatures may be found there.

The available energy of water at the point of nucleation, with respect to saturated liquid at 1 atm and 100°C, was also reported in the earlier review. These results were computed using Karimi's equation of state, which we now know to be questionable below 150°C. For the present paper, we repeated Karimi's calculation with Vandermarliere's T-cubics [22], supplemented with the  $c_p^o(T)$  correlation of Wooley [26].

To obtain the extreme limits of the damage potential, we consider two cases. In the first case, we assume that nucleation takes place at the saturated liquid state. In the second, we assume that the depressurization follows the isentropic curve drawn through the saturated liquid states, and that nucleation takes place at the intersection of this curve with the liquid spinodal line. In practice, the actual point of nucleation lies somewhere between these limits, and the pressure undershoot below the saturation pressure can be computed as a function of the saturation state and the depressurization rate using the correlation of Alamgir, Kan and Lienhard [2], which applies in the range

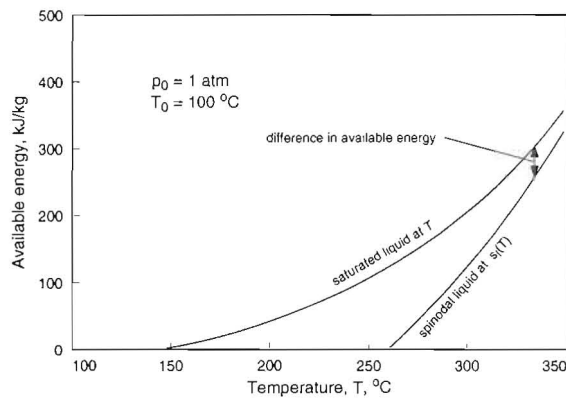


Fig. 15. Damage causing potential of water at (a) saturation and (b) spinodal points.

$0.62 < T_r < 0.93$  and depressurization rates between 400 MPa/s and  $0.15 \times 10^6$  MPa/s.

The results of the calculation are shown in fig. 15, which shows the damage potential as a function of the saturation temperature. The results of the recalculation agree with the older results of Karimi. They show that even though the pressure may fall considerably below saturation before nucleation occurs, the available energy at the nucleation point is only slightly less than that at the saturation point at which the depressurization began, even at depressurization rates as high as 0.15 MPa/s. Furthermore, this destructive availability can be as high as 300 kJ/kg. Thus the drop in pressure from saturation to nucleation does little to diminish the available energy. Rather, it is the initial temperature of the liquid that is the key factor affecting the available energy. This calculation confirms our worst fears that thermohydraulic explosions can cause enormous damage.

## 6. Summary

We need thermodynamic data in ranges of temperature and pressure which we can expect fluids to reach in engineering equipment, but these ranges can be inaccessible to measurement. Obtaining design information for such purposes entails application of thermodynamic principles and computational techniques to create such data. The important points that emerge from our discussion are:

- The key to obtaining derived thermodynamic properties is the availability of a cubic-like, accurate,  $p-v-T$  equation of state. The key to accuracy in such an equation is to impose no restriction on the temperature-dependence of its coefficients.
- Remarkably high accuracy is possible from the use of simple cubic equations. Such T-cubic equations can be developed using few but accurate stable-state properties, and the coefficients of the cubic are obtained without time-consuming regression calculations involving massive data. Our equation shows high accuracy everywhere except for superheated vapor, and even there it is tolerable.
- No data other than  $p-v-T$  and  $c_p^\circ$  are needed to develop T-cubic equations. However, if such additional data are available, they serve as a check on the fitting procedure and on the accuracy of the input  $p-v-T$  data.
- The coefficients of the T-cubic vary with temperature in a way that is hard to correlate accurately. This explains why older cubic equations, with their

temperature-dependence preconceived, have earned a reputation for inaccuracy. It is extremely difficult to write a *global* cubic that is accurate.

- The Van der Waals surface tension equation is a very stringent test of the correctness of an equation of state. T-cubic equations pass this test consistently. The equation thus enables us to obtain the surface tension data for a saturated fluid from a single experimental measurement, if available, or from a corresponding states correlation.
- A volume transformation rule has been described. With the help of this rule, existing equations of state can be transformed to give more accurate density values without affecting their vapor-liquid equilibrium predictions.
- Global cubic equations can be developed successfully by fitting the T-cubic coefficients as functions of temperature, but the computational effort is not justified by the result. Computing a table of coefficients over a range of temperatures, as a preliminary step in a calculation that needs thermodynamic property input, is more convenient and efficient.
- The T-cubic equation can be applied to create predictions and corresponding-states correlations of compressibility factor, spinodal curves, surface tension and other such derived properties.
- The specific heat at constant pressure,  $c_p$ , approaches infinity along an isobar in inverse proportion to the square root of the temperature deviation from the spinodal state. The proportionality factor in this relation is nearly constant at moderate and low pressures, and correlates well with the Pitzer factor,  $\omega$ .
- Knowledge of the approach of  $c_p$  to infinity allows us to calculate the difference between the spinodal point and the homogeneous nucleation limit. This calculation shows that the two differ by less than 1°C for water, so that we may accept the spinodal line as a stand-in for the absolute limit of homogeneous nucleation.

## Acknowledgements

Much of the work reviewed here was the result of inquiries supported by the Electric Power Research Institute through contracts to the University of Kentucky and the University of Houston. The University of Houston Energy Laboratory has also provided support. Dr. S. Sankaran performed some preliminary calculations on the  $c_p$  question. This paper would not have

been possible without a large and dedicated effort by our many co-authors in the cited papers.

## Nomenclature

### Symbols

$a$	available energy, $\equiv h - T_n s$ or $h - T_0 s$ ;
$A$	coefficient in eq. (11),
$A_0$	coefficient in eq. (22),
$c_p, c_v$	low pressure value of $A$ ,
	specific heats at constant pressure, constant volume,
$b, c, d$	coefficients in cubic equation, eq. (10),
$e$	coefficient in eq. (11),
$f$	Helmholtz function, $\equiv u - Ts$ ,
$g$	Gibbs free energy,
$h$	specific enthalpy,
$j$	number of nucleation events/number of molecular collisions,
$k$	Boltzmann's constant,
$m$	mass of a molecule,
$n$	exponent in eq. (16),
$N$	number of molecules in a nucleation event,
$p$	pressure,
$p_0, p_1$	auxiliary pressure functions, eq. (2) and eq. (3),
$r$	volume variable, section 3.1,
$R$	ideal gas constant,
$s$	specific entropy,
$T$	temperature,
$u$	specific internal energy,
$v$	specific volume,
$z$	compressibility factor, $\equiv pv/RT$ ,
$\beta$	coefficient of volume expansion at constant pressure,
$\kappa_T$	coefficient of isothermal compressibility,
$\Delta G$	critical work to create a nucleus bubble,
$\sigma$	surface tension,
$\omega$	Pitzer's acentric factor, $\equiv -1 - \log_{10}(p_{r,sat})_{T_r=0.7}$ .

### Subscripts

$a$	compressed liquid at high pressure,
$c$	critical state,
$f$	saturated liquid,
$g$	saturated vapor,
$l$	liquid spinodal point,
$m$	state in unstable region with same $T$ and $p$ as states $f$ and $g$ ,

$n$	homogeneous nucleation limit,
$r$	reduced variable,
sat	saturation,
$v$	vapor spinodal point,
0	reference value; value in ideal gas state.

### Superscripts

'	dummy variables in integrals; dimensional coefficients,
°	ideal gas state, typically $p = 1$ atm.

### Abbreviations

CEOS	continuous EOS,
CSC	corresponding-states correlation,
EOS	equation of state (usually $p-v-T$ ),
FEOS	fundamental EOS,
r.m.s.	root mean square,
T-cubic	cubic fitted isotherm by isotherm.

### References

- [1] J.H. Lienhard, N. Shamsundar and P.O. Biney, Spinodal Lines and Equations of State—a review, *Nucl. Engng. Des.* 95 (1986) 297–313.
- [2] Md. Alamgir, C.Y. Kan and J.H. Lienhard, An experimental study of the rapid depressurization of hot water, *J. Heat Transf.* 103 (1981) 52–55.
- [3] C.T. Avedisian, The homogeneous nucleation limit of liquids, *J. Phys. Chem. Ref. Data* 14 (1985) 695–729.
- [4] Q. Zheng, D.J. Durben, G.H. Wolf and C.A. Angell, Liquids at large negative pressures: water at the homogeneous nucleation limit, *Science*, 254 (1991) 829–832.
- [5] V.P Skripov, *Metastable Liquids* (1970), English translation (John Wiley and Sons, New York, 1974).
- [6] R.C. Reid, J.M. Prausnitz and B.E. Poling, *The Properties of Gases and Liquids* (McGraw-Hill, New York, 1987).
- [7] S.M. Walas, *Phase Equilibria in Chemical Engineering* (Butterworth, Boston, 1985).
- [8] J.H. Keenan, F.G. Keyes, P.G. Hill and J.G. Moore, *Steam Tables* (John Wiley and Sons, New York, 1969).
- [9] L. Haar and J.S. Gallagher, Thermodynamic properties of ammonia, *J. Phys. Chem. Ref. Data* 7 (1978) 635–788.
- [10] L. Haar, J.S. Gallagher and G.S. Kell, Thermodynamic properties for fluid water, in: *Water and Steam*, Eds. J. Straub and K. Scheffler (Pergamon Press, New York, 1980) 69–72.
- [11] B.A. Younglove, *Thermophysical Properties of Fluids 1. Argon, Ethylene, Parahydrogen, Nitrogen, Nitrogen Trifluoride and Oxygen*, *J. Phys. Chem. Ref. Data* 11, Sup. 1 (1982).

- [12] L. Haar, J.S. Gallagher and G.S. Kell, NBS/NRC Steam Tables (Hemisphere Pub. Co., New York, 1984).
- [13] J.D. van der Waals, Thermodynamische Theorie der Kapillarität unter Voraussetzung stetiger Dichteänderung, Zeit. Phys. Chem. 13 (1894) 657–725.
- [14] International Formulation Committee, A formulation of the thermodynamic properties of ordinary water and thermodynamic properties of ordinary water substance calculated from the 1968 IFC formulation for scientific use, 1969 (ASME, New York).
- [15] N. Shamsundar and R.P. Reddy, An invariance property associated with  $p-v-T$  equations of state, Ind. Eng. Chem. Res. 30 (1991) 2168–2172.
- [16] G. Soave, Equilibrium constants from a modified Redlich-Kwong equation of state, Chem. Eng. Sci. 27 (1972) 1197–1203.
- [17] G.S. Soave, Application of a cubic equation of state to vapour-liquid equilibria of systems containing polar compounds, Inst. Chem. Engr. Symp. Ser. 56 (1979) 1.2/1–1.2/16.
- [18] R.E. Peck, The assimilation of van der Waals' equation in the corresponding states family, Can. J. Chem. Eng. 60 (1982) 446–449.
- [19] W.C. Reynolds, Thermodynamic Properties in SI (Department of Mech. Eng., Stanford Univ., 1979).
- [20] C.S. Murali, Cubic equation of state for water, hydrocarbons and liquid metals, MSME Thesis, Dept. of Mech. Eng., Univ. of Houston (1984).
- [21] P.O. Biney, A new fundamental thermodynamic equation representing water in stable, metastable and unstable states, PhD Dissertation, Dept. Mech. Eng., Univ. of Houston (1987).
- [22] P. Vandermarliere, Global cubic equation of state for thermodynamic properties, MSME Thesis, Dept. of Mech. Eng., Univ. of Houston (1988).
- [23] R.P. Reddy, Cubic thermodynamic  $p-v-T$  equations and a modified corresponding states principle, PhD Dissertation, Dept. of Mech. Eng., Univ. of Houston (1991).
- [24] A. Karimi, A fundamental equation representing water in the stable, metastable and unstable states, PhD Dissertation, Dept. of Mech. Eng., Univ. of Kentucky (1982).
- [25] A. Harmens and H. Knapp, Three-parameter cubic equation of state for normal substances, Ind. Eng. Chem. Fund. 19 (1980) 291–294.
- [26] H.W. Wooley, Thermodynamic properties of for  $H_2O$  in the ideal gas state, in Water and Steam, J. Straub and K. Scheffler, eds. (Pergamon Press, Oxford, 1980) 166.
- [27] W-g. Dong and J.H. Lienhard, Corresponding-states correlation of saturated and metastable properties, Canadian J. Chem. Eng. 64 (1986) 158–161.
- [28] B.I. Lee and M.G. Kesler, A generalized thermodynamic correlation based on three-parameter corresponding states, AIChE J. 21 (1975) 510–527.
- [29] N.B. Vargaftik, Tables of Thermophysical Properties of Liquids and Gases, 2nd Ed. (Hemisphere Publishing Co., Washington, 1975).
- [30] P.O. Biney, W-g. Dong and J.R. Lienhard, Use of a cubic equation of state to predict surface tension and spinodal limits, J. Heat Transf. 108 (1986) 405–410.
- [31] J.R. Lienhard and A. Karimi, Homogeneous nucleation and the spinodal line, J. Heat Transf. 103 (1981) 61–64.
- [32] J. Frenkel, Kinetic Theory of Liquids (Dover Pub., New York, 1955).
- [33] J.H. Lienhard and A. Karimi, Corresponding states correlations of the extreme liquid superheat and vapor subcooling, J. Heat Transf. 100 (1978) 492–495.